INSTITUTE OF PHYSICS PUBLISHING JOURNAL OF PHYSICS B: ATOMIC, MOLECULAR AND OPTICAL PHYSICS

J. Phys. B: At. Mol. Opt. Phys. **38** (2005) 23–42 doi:10.1088/0953-4075/38/1/003

Two-electron photoemission from polarized atoms

J Berakdar[1] **and N M Kabachnik**[1,2,3]

[1] Max-Planck Institut für Mikrostrukturphysik, 06120 Halle, Germany
[2] Fakultät für Physik, Universität Bielefeld, 33615 Bielefeld, Germany

Received 18 October 2004
Published 17 December 2004
Online at stacks.iop.org/JPhysB/38/23

Abstract

Double ionization of a polarized atom by a single photon with an arbitrary polarization is theoretically considered. A general expression for the triple differential cross section is obtained and analysed. We point out the existence of a circular and a linear dichroism in the angular distributions of photoelectrons. Generally two types of sources for the dichroism are distinguished: one connected with the initial polarization of the target, and the other related to the two-electron final-state properties. We show how these two types of dichroic effects can be experimentally investigated separately by choosing the detection geometry appropriately. As an example, the photo-double ionization of 2P excited and polarized states of atomic helium is considered. The calculations reveal a measurable dichroism in the angular correlations of two emitted electrons. Possible applications of circular dichroism measurements to the study of superconductors and orbitally ordered materials are discussed.

(Some figures in this article are in colour only in the electronic version)

1. Introduction

The process of two-electron emission following the absorption of a single vacuum ultraviolet photon by an atom, widely referred to as the process of photo-double ionization (PDI), has been under intensive theoretical and experimental investigations, in particular during the last decade. The interest in this process is mainly driven by the fact that PDI involves inevitably some sort of electron–electron correlations, for the electron–photon operator is of a single particle nature. The premise is therefore to gain detailed information on the electronic correlations by studying the PDI processes [1, 2]. Experimentally, the progress in studying PDI depends crucially on the availability of high-brilliance synchrotron radiation sources and on the development of efficient coincidence techniques. In both of these respects major advances have been made in recent years with the result that nowadays, a wealth of experimental data have been accumulated mostly for the He atom (for a review see [2] and references therein). Other noble gas [3, 4] and alkaline-earth atoms [5, 6] have been

[3] Permanent address: Institute of Nuclear Physics, Moscow State University, 119992 Moscow, Russia.

studied by means of PDI as well. This impressive progress on the experimental side has been accompanied by considerable theoretical efforts using various theoretical approaches, ranging from simple model and approximate wavefunction calculations [4, 7–9] to fully-fledged numerical evaluations of the cross sections [10–12]. At this stage of development, one is therefore tempted to conclude that most of the features of PDI from the *ground state* of simple targets (such as He) are currently sufficiently well understood. On the other hand, PDI studies from more complex systems, such as large molecules, clusters and condensed matter are still in their infancy. The PDI in this case may serve as a unique tool to map out some of the aspects of the screened (non-local and frequency-dependent) electron–electron interaction in the presence of a polarizable medium. Some steps in this direction have been made recently, in particular for solid surfaces [13–15], for superconductors [16] and for fullerenes [17–19].

To our knowledge all investigations of PDI have been done for unpolarized targets. On the other hand, recalling the historical development of single photoionization studies, one can say that utilizing polarized targets increased substantially the amount of information experimentally obtainable and gave access to a new sort of phenomena. For example, in atomic physics the study of angular distributions of photoelectrons produced via photoionizing polarized atoms [20–23] offers the possibility of realizing what is called the complete experiment. Such experiments deliver information on the amplitudes for the photoionization process including their phases [21]. In solid state physics the study of photoelectron emission from (spin) polarized targets yields, for example, valuable information on the local magnetization [24]. Thus, it is natural to raise the question as to what information can be gained by studying PDI from polarized targets. It is the aim of this work to address this problem and to provide a realistic estimate of the related cross sections which is important in judging the experimental feasibility of such measurements.

The paper is organized as follows: in the next section the general expression for the PDI cross section is obtained for polarized atoms. Section 3 is devoted to the discussion of the different types of dichroism which are inherent to the PDI from polarized targets. In section 4 we discuss the general properties of the circular dichroism (CD) and derive explicit results for the CD within the plane wave approximation (PWA). This enables us to reveal the kind of information that may be extracted from the measurements of PDI of oriented targets. In section 5 as an illustration we present the results of our calculations of PDI for the simplest possible two-electron system, namely the excited and polarized He atom. In section 6 we shortly discuss possible applications of the phenomenon of circular dichroism in PDI to the problems of superconductors. In the last section some conclusions and further suggestions are given. Atomic units are used throughout unless otherwise indicated.

2. General theory

We consider double ionization of atoms by a single photon with an arbitrary polarization. The initial state of the atom is characterized by a certain energy E_0, a total angular momentum J_0, a projection of the angular momentum M_0, and a set of other quantum numbers which we denote by α_0. Similarly, the final ionic state is determined by E_f, α_f, J_f, M_f. The two emitted electrons are characterized by their momenta $\mathbf{p}_1, \mathbf{p}_2$ and spin projections σ_1, σ_2. The energies of the two detected electrons, E_1 and E_2, are constrained by the energy conservation

$$E_1 + E_2 = E_\gamma + E_0 - E_f, \tag{1}$$

where E_γ is the photon energy. The transition amplitude for PDI has the form

$$T_{\hat{\epsilon}}(\mathbf{p}_1, \mathbf{p}_2) = \hat{\epsilon} \cdot \mathbf{f}(\mathbf{p}_1, \mathbf{p}_2), \tag{2}$$

$$\mathbf{f}(\mathbf{p}_1, \mathbf{p}_2) = \langle \alpha_f J_f M_f, \mathbf{p}_1\sigma_1, \mathbf{p}_2\sigma_2 | \mathbf{D} | \alpha_0 J_0 M_0 \rangle, \tag{3}$$

where $\hat{\boldsymbol{\epsilon}}$ is the polarization vector of the photon, and $\mathbf{D}$ is the dipole operator. In the following we use the density matrix of the initial atomic state $\rho^i(J_0)$ and the density matrix $\rho^f(J_f, \mathbf{p}_1, \mathbf{p}_2)$ of the final state consisting of the residual ion and the two emitted electrons. The two density matrices are connected to each other via the T-operator: $\rho^f(J_f, \mathbf{p}_1, \mathbf{p}_2) = T_{\hat{\boldsymbol{\epsilon}}} \rho^i(J_0) T^+_{\hat{\boldsymbol{\epsilon}}}$. The fully differential cross section for PDI depends on the momentum vectors $\mathbf{p}_1$ and $\mathbf{p}_2$. Assuming E_f is known (in addition to $E_{1,2}$ and E_γ) one usually utilizes equation (1) and writes the cross section in terms of the solid angles $\Omega_{1,2}$ of $\mathbf{p}_{1,2}$ and the energy E_1 of one of the emitted electrons (therefore the cross section is referred to as the triple differential cross section). Mathematically, the cross section is the trace over the final state density matrix, i.e.

$$\frac{\mathrm{d}^3\sigma}{\mathrm{d}\Omega_1\,\mathrm{d}\Omega_2\,\mathrm{d}E_1} = c\,\mathrm{Tr}\,\rho^f = c\,\mathrm{Tr}\left(T_{\hat{\boldsymbol{\epsilon}}}\rho^i T^+_{\hat{\boldsymbol{\epsilon}}}\right) = c\,\mathrm{Tr}\,(\mathbf{D}\rho^\gamma \rho^i \mathbf{D}^+). \tag{4}$$

Here $\rho^\gamma = \hat{\boldsymbol{\epsilon}} \cdot \hat{\boldsymbol{\epsilon}}'^*$ is the density matrix of the photon, and c is a kinematical normalization constant which is specified below. Equation (4) is expressed in an appropriately chosen basis. For the present purposes we expand equation (4) as follows:

$$\begin{aligned}\frac{\mathrm{d}^3\sigma}{\mathrm{d}\Omega_1\,\mathrm{d}\Omega_2\,\mathrm{d}E_1} = c \sum_{M_0 M_0' M_f \sigma_1 \sigma_2 \lambda\lambda'} & \langle \alpha_f J_f M_f, \mathbf{p}_1\sigma_1, \mathbf{p}_2\sigma_2 | D_\lambda | \alpha_0 J_0 M_0 \rangle \langle \lambda | \rho^\gamma | \lambda' \rangle \\ & \times \langle \alpha_0 J_0 M_0 | \rho^i | \alpha_0 J_0 M_0' \rangle \langle \alpha_f J_f M_f, \mathbf{p}_1\sigma_1, \mathbf{p}_2\sigma_2 | D_{\lambda'} | \alpha_0 J_0 M_0' \rangle^*,\end{aligned} \tag{5}$$

where the photon is described in the helicity representation. In principle, starting from equation (5) one may calculate the dipole amplitudes $\mathbf{f}(\mathbf{p}_1, \mathbf{p}_2)$ and obtain the PDI cross section. This is done in section 4 for simple systems. However, valuable information can be extracted by inspecting the general structure and symmetry properties of equation (5). To exploit the full power of the formalisms of density matrices and irreducible tensors, it is advantageous to express the polarization of the initial atomic state in terms of the statistical tensors, $\rho_{k_0 q_0}$ (state multipoles). These are related to the atomic density matrix via the formula [25–27]

$$\rho_{k_0 q_0}(\alpha_0 J_0, \alpha_0' J_0') = \sum_{M_0 M_0'} (-1)^{J_0' - M_0'} (J_0 M_0, J_0' - M_0' | k_0 q_0) \langle \alpha_0 J_0 M_0 | \rho^i | \alpha_0' J_0' M_0' \rangle, \tag{6}$$

where $(j_1 m_1, j_2 m_2 | jm)$ are the Clebsch–Gordan coefficients. In this work we consider an arbitrary atomic target having an initial state with a definite angular momentum J_0. Therefore, we write for brevity

$$\rho_{k_0 q_0}(\alpha_0 J_0) \equiv \rho_{k_0 q_0}(\alpha_0 J_0, \alpha_0 J_0).$$

The rank of the statistical tensor k_0 and the component q_0 are limited by the relations

$$0 \leqslant k_0 \leqslant 2J_0, \qquad -k_0 \leqslant q_0 \leqslant k_0.$$

In the majority of practically interesting cases the polarized initial atomic state has an axial symmetry with respect to some axis $\hat{\mathbf{a}} \equiv (\theta_a, \phi_a)$. In this case the statistical tensors of the state in the laboratory frame can be expressed as follows [27]:

$$\rho_{k_0 q_0}(\alpha_0 J_0) = \sqrt{\frac{4\pi}{2k_0 + 1}}\, Y^*_{k_0 q_0}(\theta_a, \phi_a) \bar{\rho}_{k_0 0}(\alpha_0 J_0) \tag{7}$$

where $Y_{k_0 q_0}(\theta_a, \phi_a)$ are spherical harmonics, and $\bar{\rho}_{k_0 q_0}(\alpha_0 J_0)$ are the statistical tensors in the 'atomic' frame (z'-axis along the target polarization direction $\hat{\mathbf{a}}$). The photon beam can also be characterized by statistical tensors that depend on the Stokes parameters P_1, P_2, P_3 [27],

i.e. $\rho^{\gamma}_{k_\gamma q_\gamma}(P_1, P_2, P_3)$. In the dipole approximation the rank k_γ of the photon tensors is limited to $k_\gamma \leqslant 2$.

Within the density matrix and the statistical tensor formalism the triply differential cross section of PDI, equation (4), can be presented as

$$\frac{\mathrm{d}^3\sigma}{\mathrm{d}\Omega_1\,\mathrm{d}\Omega_2\,\mathrm{d}E_1} = c\sum_{\alpha\alpha' JJ' kq} \rho^{f}_{kq}(\alpha J, \alpha' J')\varepsilon^{*}_{kq}(\alpha J, \alpha' J'). \tag{8}$$

Here $\rho^{f}_{kq}(\alpha J, \alpha' J')$ is the statistical tensor of the system consisting of the residual ion and the two electrons in the final state, $J(J')$ is the total angular momentum of the system, and $\alpha(\alpha')$ denote all other quantum numbers which are necessary to determine the final state such as the angular momentum of the ion J_f, the orbital and the total angular momenta of the emitted electrons, etc (see below). The tensor $\varepsilon_{kq}(\alpha J, \alpha' J')$ is the 'efficiency tensor' of the detector system, which we discuss later on. The summation over α, α' means summation over all unobservable quantum numbers. The statistical tensors of the final state can be expressed in terms of the statistical tensors of the initial state (atom+photon) and the reduced matrix elements of the dipole operator describing photoionization (see, e.g., [27], equation (2.117))

$$\rho^{f}_{kq}(\alpha J, \alpha' J') = \sum_{k_0 q_0 k_\gamma q_\gamma} \hat{k}_0 \hat{k}_\gamma (k_0 q_0, k_\gamma q_\gamma | kq) \begin{Bmatrix} J_0 & 1 & J \\ J_0 & 1 & J' \\ k_0 & k_\gamma & k \end{Bmatrix}$$
$$\times \rho_{k_0 q_0}(\alpha_0 J_0)\rho^{\gamma}_{k_\gamma q_\gamma}(P_1, P_2, P_3)\langle \alpha J||D||\alpha_0 J_0\rangle \langle \alpha' J'||D||\alpha_0 J_0\rangle^{*}, \tag{9}$$

where $\hat{k} \equiv (2k+1)^{1/2}$, $\langle \alpha J||D||\alpha_0 J_0\rangle$ is the reduced dipole matrix element. For the Wigner 9j-symbols we use the standard notations.

We suppose that the residual ion is not detected but both electron momentum vectors are measured. In addition, we assume, as is usually the case, that the electron detectors are not sensitive to the electron spins. Expanding the emitted electron wavefunctions in partial waves one finds for the efficiency tensor ε_{kq} in equation (8) the following expression (cf [27], equation (1.179)).

$$\varepsilon_{kq}(\alpha J, \alpha' J') = (4\pi)^{-1}(-1)^{j+j'+J_f+k+j_1'+j_2'+1}\hat{\ell}_1\hat{\ell}_1'\hat{\ell}_2\hat{\ell}_2'\hat{j}_1\hat{j}_1'\hat{j}_2\hat{j}_2'\hat{j}\hat{j}'\hat{J}\hat{J}' \begin{Bmatrix} J & j & j' \\ J' & J_f & k \end{Bmatrix}$$
$$\times \sum_{k_1 k_2} (\ell_1 0, \ell_1' 0|k_1 0)(\ell_2 0, \ell_2' 0|k_2 0) \begin{Bmatrix} \ell_1 & j_1 & \frac{1}{2} \\ j_1' & \ell_1' & k_1 \end{Bmatrix} \begin{Bmatrix} \ell_2 & j_2 & \frac{1}{2} \\ j_2' & \ell_2' & k_2 \end{Bmatrix} \begin{Bmatrix} j_1 & j_2 & j \\ j_1' & j_2' & j' \\ k_1 & k_2 & k \end{Bmatrix}$$
$$\times \{Y_{k_1}(\theta_1, \phi_1) \otimes Y_{k_2}(\theta_2, \phi_2)\}^{*}_{kq}. \tag{10}$$

Here ℓ_i, j_i $(i = 1, 2)$ are the orbital and the total angular momenta of the ith electron. In fact ℓ_i and j_i are included in the index α and summation over α in equation (8) means summation over ℓ_i and j_i. $\{Y_{k_1}(\theta_1, \phi_1) \otimes Y_{k_2}(\theta_2, \phi_2)\}_{kq}$ are bipolar harmonics [28] determined as the tensor product of two spherical harmonics

$$\{Y_{k_1}(\theta_1, \phi_1) \otimes Y_{k_2}(\theta_2, \phi_2)\}_{kq} = \sum_{q_1, q_2} (k_1 q_1, k_2 q_2|kq) Y_{k_1 q_1}(\theta_1, \phi_1) Y_{k_2 q_2}(\theta_2, \phi_2) \tag{11}$$

where $\hat{\mathbf{n}}_i \equiv (\theta_i, \phi_i)$ is the direction of emission of the ith electron. We use the coupling scheme $\mathbf{J_f} + (\mathbf{j_1} + \mathbf{j_2})\mathbf{j} = \mathbf{J}$ where j is the total angular momentum of the electron pair.

Substituting formulae (9) and (10) into equation (8) and making use of equation (7) we obtain for the triple differential cross section of photo-double ionization the compact expression

$$\frac{\mathrm{d}^3\sigma}{\mathrm{d}\Omega_1\,\mathrm{d}\Omega_2\,\mathrm{d}E_1} = \pi\alpha E_\gamma (3\hat{J}_0)^{-1} \sum_{k_1k_2k_0k_{k_\gamma}} \bar{\rho}_{k_00}(\alpha_0 J_0) B^{k_1k_2}_{k_0kk_\gamma} F^{k_1k_2}_{k_0kk_\gamma}. \tag{12}$$

Here the normalization factor is chosen in such a way that for unpolarized atoms upon integration over the emission angles of both electrons one obtains the conventional expression for total cross section [29]; α is the fine-structure constant. $F^{k_1k_2}_{k_0kk_\gamma}$ is a kinematical factor which depends only on the kinematics of the experiment as set by the chosen experimental arrangement of $\hat{\mathbf{a}}$, $\hat{\mathbf{n}}_1$ and $\hat{\mathbf{n}}_2$ and the polarization of the photon beam. Its explicit form reads

$$F^{k_1k_2}_{k_0kk_\gamma} = \sqrt{4\pi}\big(\big\{Y_{k_0}(\hat{\mathbf{a}}) \otimes \big\{Y_{k_1}(\hat{\mathbf{n}}_1) \otimes Y_{k_2}(\hat{\mathbf{n}}_2)\big\}_k\big\}_{k_\gamma} \cdot \rho^{\gamma *}_{k_\gamma}(P_1, P_2, P_3)\big). \tag{13}$$

Here $(a_k \cdot b_k)$ and $\{a_k \otimes b_k\}$ stand respectively for the scalar [28] and tensor (cf equation (11)) product of the two spherical tensors a_k and b_k. Thus, $\big\{Y_{k_0}(\hat{\mathbf{a}}) \otimes \big\{Y_{k_1}(\hat{\mathbf{n}}_1) \otimes Y_{k_2}(\hat{\mathbf{n}}_2)\big\}_k\big\}_{k_\gamma q_\gamma}$ are tripolar harmonics [28]. The selection rules inherent to the Clebsch–Gordan coefficients in $F^{k_1k_2}_{k_0kk_\gamma}$ limit substantially the range of indices in the summation present in equation (12).

The dynamics of the process is encompassed in the coefficients $B^{k_1k_2}_{k_0kk_\gamma}$ which depend on the dipole matrix elements of photoionization, specifically $B^{k_1k_2}_{k_0kk_\gamma}$ has the form

$$\begin{aligned} B^{k_1k_2}_{k_0kk_\gamma} = {} & 3\hat{J}_0\hat{k}(-1)^{1+k_0+k+J_f} \sum_{jj'JJ'} \sum_{j_1j_2j_1'j_2'} (-1)^{j_1'+j_2'+j'+J} \hat{j}\hat{j}'\hat{J}\hat{J}'\hat{j}_1\hat{j}_1'\hat{j}_2\hat{j}_2'\hat{\ell}_1\hat{\ell}_1'\hat{\ell}_2\hat{\ell}_2' \\ & \times (\ell_1 0, \ell_1' 0|k_1 0)(\ell_2 0, \ell_2' 0|k_2 0) \begin{Bmatrix} J & j & J_f \\ j' & J' & k \end{Bmatrix} \begin{Bmatrix} \ell_1 & j_1 & \frac{1}{2} \\ j_1' & \ell_1' & k_1 \end{Bmatrix} \begin{Bmatrix} \ell_2 & j_2 & \frac{1}{2} \\ j_2' & \ell_2' & k_2 \end{Bmatrix} \begin{Bmatrix} J_0 & 1 & J \\ J_0 & 1 & J' \\ k_0 & k_\gamma & k \end{Bmatrix} \\ & \times \begin{Bmatrix} j_1 & j_2 & j \\ j_1' & j_2' & j' \\ k_1 & k_2 & k \end{Bmatrix} \langle J_f(j_1j_2)j : J||D||J_0\rangle \langle J_f(j_1'j_2')j' : J'||D||J_0\rangle^*. \end{aligned} \tag{14}$$

Due to parity conservation the sum $\ell_1 + \ell_2$ can only be even or only odd, meaning that the condition

$$k_1 + k_2 = \text{even}$$

applies. Integrating over the angles of one of the electrons one obtains

$$\int F^{k_1k_2}_{k_0kk_\gamma}\,\mathrm{d}\Omega_1 = \delta_{k_10}\delta_{k_2k} F_{k_0kk_\gamma},$$

where $F_{k_0kk_\gamma}$ is the geometrical factor introduced by Baier *et al* [30] for the single photoionization of polarized atoms. Furthermore, averaging over all target polarization directions (i.e., for unpolarized targets, $k_0 = 0$) one deduces the formula

$$F^{k_1k_2}_{0kk_\gamma} = \delta_{kk_\gamma}\big(\big\{Y_{k_1}(\hat{\mathbf{n}}_1) \otimes Y_{k_2}(\hat{\mathbf{n}}_2)\big\}_{k_\gamma} \cdot \rho^{\gamma *}_{k_\gamma}(P_1, P_2, P_3)\big).$$

In this case the triple differential cross section can be presented in a form identical to that given in [31]

$$\frac{\mathrm{d}^3\sigma}{\mathrm{d}\Omega_1\,\mathrm{d}\Omega_2\,\mathrm{d}E_1} = \pi\alpha E_\gamma (3\hat{J}_0^2)^{-1} \sum_{k_1k_2k_\gamma} A_{k_1k_2k_\gamma}\big(\big\{Y_{k_1}(\hat{\mathbf{n}}_1) \otimes Y_{k_2}(\hat{\mathbf{n}}_2)\big\}_{k_\gamma} \cdot \rho^{\gamma *}_{k_\gamma}(P_1, P_2, P_3)\big) \tag{15}$$

where $A_{k_1k_2k_\gamma} = B^{k_1k_2}_{0k_\gamma k_\gamma}$.

It is useful to inspect some symmetry properties of the dynamical coefficients $B^{k_1k_2}_{k_0kk_\gamma}$. Permutation of primed and non-primed angular momenta results in a phase factor and a complex conjugation, therefore

$$B^{k_1k_2}_{k_0kk_\gamma} = (-1)^{k_0+k_\gamma}\left(B^{k_1k_2}_{k_0kk_\gamma}\right)^*.$$

Hence, if $k_0 + k_\gamma =$ even, the B coefficients are real, whereas if $k_0 + k_\gamma =$ odd, the B coefficients are purely imaginary.

For light atoms the LS-coupling approximation is appropriate. Within the LS-coupling scheme, expression (14) is reduced to

$$\begin{aligned} B^{k_1k_2}_{k_0kk_\gamma} = 3\hat{L}_0\hat{k}(-1)^{k_0+k+L_f} \sum_{\bar{S}\bar{L}\bar{L}'LL'} \sum_{\ell_1\ell_2\ell_1'\ell_2'} (-1)^{\ell_1'+\ell_2'+\ell'+L}\hat{\bar{L}}\hat{\bar{L}}'\hat{L}\hat{L}'\hat{\ell}_1\hat{\ell}_1'\hat{\ell}_2\hat{\ell}_2' \\ \times (\ell_1 0, \ell_1' 0|k_1 0)(\ell_2 0, \ell_2' 0|k_2 0)\begin{Bmatrix} L & \bar{L} & L_f \\ \bar{L}' & L' & k \end{Bmatrix}\begin{Bmatrix} L_0 & 1 & L \\ L_0 & 1 & L' \\ k_0 & k_\gamma & k \end{Bmatrix}\begin{Bmatrix} \ell_1 & \ell_2 & \bar{L} \\ \ell_1' & \ell_2' & \bar{L}' \\ k_1 & k_2 & k \end{Bmatrix} \\ \times \langle L_f S_f(\ell_1\ell_2)\bar{L}\bar{S} : L||D||L_0S_0\rangle\langle L_f S_f(\ell_1'\ell_2')\bar{L}'\bar{S} : L'||D||L_0S_0\rangle^*. \end{aligned} \tag{16}$$

Here $\bar{L}$ and $\bar{S}$ denote the orbital angular moment and the spin of the electron pair, whereas $\langle L_f S_f(\ell_1\ell_2)\bar{L}\bar{S} : L||D||L_0S_0\rangle$ is the reduced dipole matrix element in the LS-coupling approximation. Since the dipole operator does not act on spin variables, the spin is conserved: $\mathbf{S_f} + \bar{\mathbf{S}} = \mathbf{S_0}$.

The derived expressions (12)–(14) and (16) can be used in direct calculations of the PDI triple differential cross section provided the dipole amplitudes are calculated. On the other side, they may be used for a qualitative analysis. Thus in order to analyse the possible contributions from different parts of the target density matrix (different statistical tensors) it is very convenient to consider the kinematical factor $F^{k_1k_2}_{k_0kk_\gamma}$. This serves also as an indicator for choosing the suitable geometry of the experiment that is appropriate for studying certain goals. We apply such analysis in the next section considering different types of dichroism.

3. Dichroism

The analysis of PDI data based on the general expression (12) for the triple differential cross section is a rather formidable task. In practice, it is often more convenient to consider not the cross section itself but differences of cross sections corresponding to different polarization states of the photon beam or of the target. These kinds of cross-section differences are conventionally referred to as *dichroism*. Often a study of dichroism is not only convenient but very informative as well since the dichroism is related to certain physical properties of the studied system usually connected with its symmetry. Various types of dichroism were studied in single photoionization of polarized targets (see, e.g., [22] and references therein). For a fixed target polarization one can consider, for instance, the difference in the cross sections for right and left circularly polarized light. This difference defines what is called the *circular dichroism*. In single photoionization of atoms the existence of the CD is a signature of the presence of a preferential orientation direction of the target. We emphasize, however, that also an alignment of the target atom results in a finite CD in angular-resolved experiments [22]. If linearly polarized light is used one can consider the difference in the cross sections for two mutually perpendicular axis along which the light polarization vector (or the electric-field vector) is aligned. This difference is labelled usually as the *linear dichroism* (LD). Since we will be dealing in this paper with angle-resolved experiments only we will always encounter dichroism effect in angular distribution (AD). We remark in this context that the standard

abbreviations CDAD and LDAD are shortened to CD and LD in this work. We note also that from the point of view of symmetry the DPI of oriented atoms is similar to that of diatomic (linear) molecules, where CD and LD were discussed as well [32, 33]. Many features of the dichroism are therefore alike for diatomic molecules and for oriented and/or aligned atoms.

A further important kind of dichroism is obtained when, for a fixed polarization of the photon beam, the direction of the target polarization is changed [34]. If circularly polarized light is used and the direction of target orientation is reversed, the resulting dichroism is called *circular magnetic dichroism* (CMD), similarly if linearly polarized light is employed one studies then the *linear magnetic dichroism* (LMD). Finally, if the target is aligned one can study the photoionization with (fixed) linearly polarized light and two perpendicular directions of target alignment which yields the *linear alignment dichroism* (LAD) [35]. In all the cases the advantage of the dichroism studies is that only few terms of the sum (12) contribute to the difference of the cross sections, and we can focus on the influence of the existence of a particular axis or direction on the photoionization process.

In the case of single photoionization of atoms all kinds of dichroism are rooted in a polarization (i.e. orientation or/and alignment) of the target. If the target atom is unpolarized the dichroism vanishes. In general, this type of *polarization dichroism* is anticipated to occur in double ionization as well, but the information contained in the polarization dichroism in PDI is different from that appearing in single photoionization. We will elaborate on this point below. On the other hand, in double photoionization there exists a certain type of circular dichroism which is related to phase relations within the final-state two-electron wavefunction [36]. Since the final state wavefunction depends (parameterically) on the experimentally measurable momenta $\mathbf{p}_{1,2}$ this dichroism is observable by measuring the two-electron energy and/or angular distributions even for unpolarized targets [9, 37]. Such type of CD was predicted for direct PDI [9] and experimentally observed for PDI of He [38–40]. Similar CD effect was predicted for the resonant PDI [31] and experimentally confirmed in the two-step PDI of Xe [41]. This CD is not determined by the intrinsic chiral properties of the target in the initial state but rather by the chirality of the emitted electron pair moving in the field of the residual ion. Hence, the CD is dependent on the choice of the experimental conditions and therefore we call it hereafter *kinematical dichroism*. The kinematical dichroism vanishes when the emitted electron pair loses its chirality, i.e. when electrons are emitted in one or opposite directions, or have equal energies. Additionally it vanishes when the photon beam direction and both emission directions are coplanar [9]. The kinematical conditions under which the kinematical dichroism vanishes are called in this work *non-chiral kinematics*. Obviously, both polarization dichroism and kinematical dichroism should be present in PDI of polarized atoms. Below we discuss some properties of dichroism in PDI. As an illustration we consider an initial atomic state with $J_0 = 1$. In this case the atom may be aligned ($\bar{\rho}_{20} \neq 0$) or oriented ($\bar{\rho}_{10} \neq 0$). We note that an oriented target with $J_0 > 1/2$ has always nonzero alignment ($\bar{\rho}_{20} \neq 0$). Thus the rank of the statistical tensors in the considered initial state is limited to $k_0 = 0, 1, 2$.

3.1. Circular dichroism

The circular dichroism, CD, is defined as the following difference:

$$\mathrm{CD} = \left.\frac{\mathrm{d}^3\sigma}{\mathrm{d}\Omega_1\,\mathrm{d}\Omega_2\,\mathrm{d}E_1}\right|_{+} - \left.\frac{\mathrm{d}^3\sigma}{\mathrm{d}\Omega_1\,\mathrm{d}\Omega_2\,\mathrm{d}E_1}\right|_{-} \tag{17}$$

of the cross sections for right (+) and left (−) circularly polarized light (a convention is used in which a right (left) circularly polarized light has $\hat{\epsilon}_+$ ($\hat{\epsilon}_-$) polarization vector). The

z-axis is chosen to be along the photon beam. Evidently, upon substituting the sum (12) into the definition (17) only terms containing the photon tensor ρ^{γ}_{10} survive, for this tensor is proportional to the P_3 Stokes parameter which changes the sign for right and left circularly polarized light. Thus, only the dynamical coefficients $B^{k_1k_2}_{k_0kk_\gamma=1}$ contribute to CD. If the target is unpolarized ($k_0 = 0$) only the subset $B^{k_1k_2}_{011}$ is relevant to the CD. In this case one can show that $k_1 = k_2$, and the coefficients $B^{k_1k_1}_{011}$ are purely imaginary [9]. Using a technique developed by Manakov *et al* [42] for the reduction of bipolar harmonics one can show that the corresponding kinematical factors F^{kk}_{011} are proportional to the mixed product $(\hat{\mathbf{n}}_\gamma \cdot [\hat{\mathbf{n}}_1 \times \hat{\mathbf{n}}_2])$ where $\hat{\mathbf{n}}_\gamma$ is a unit vector directed along the photon beam. This is a typical kinematical dichroism. It vanishes in the non-chiral kinematics of the experiment. It also disappears upon integration over the direction of one or both electrons.

If the target is oriented ($k_0 = 1, 2$) CD is generally nonzero even for the total (integrated) cross section which is governed by the coefficient B^{00}_{101}. On the other hand, the coefficients $B^{k_1k_2}_{1k1}$ and $B^{k_1k_2}_{2k1}$ determine CD in the angular distribution; the corresponding terms in the cross section contain as factors the degree of orientation $\bar{\rho}_{10}$ and the degree of alignment $\bar{\rho}_{20}$ of the initial state, respectively. We remark that in this case the kinematical dichroism is also present; in order to study the target polarization one should therefore choose a non-chiral kinematics so that the kinematical dichroism is eliminated (e.g., a coplanar geometry where $\hat{\mathbf{n}}_\gamma$, $\hat{\mathbf{n}}_1$ and $\hat{\mathbf{n}}_2$ are in one plane). The maximal CD effect is expected when the target orientation vector is parallel to the photon beam ($\hat{\mathbf{a}} \parallel \hat{\mathbf{n}}_\gamma$).

If the target is only aligned (i.e. for $k_0 = 2$) the CD is still nonzero even if the kinematical dichroism vanishes. The alignment-induced dichroism is governed by the coefficients $B^{k_1k_2}_{2k1}$ which are purely imaginary. CD for aligned atoms is nonzero after integration over the emission angles of one of the electrons, but vanishes in total cross section (integrated over both solid angles of the emitted electrons). As clear from the analysis of $F^{k_1k_2}_{2k1}$ the CD associated with the atom alignment vanishes in non-chiral kinematics when additionally $\hat{\mathbf{a}} \parallel \hat{\mathbf{n}}_\gamma$ or if any three of four vectors $\hat{\mathbf{n}}_\gamma$, $\hat{\mathbf{n}}_1$, $\hat{\mathbf{n}}_2$ and $\hat{\mathbf{a}}$ are collinear.

3.2. Magnetic dichroism

Suppose the target is oriented and one is interested in the magnetic dichroism (MD), i.e. in the difference of the photoionization cross sections for opposite directions of the target orientation vector

$$\mathrm{MD} = \left.\frac{\mathrm{d}^3\sigma}{\mathrm{d}\Omega_1\,\mathrm{d}\Omega_2\,\mathrm{d}E_1}\right|_{\uparrow} - \left.\frac{\mathrm{d}^3\sigma}{\mathrm{d}\Omega_1\,\mathrm{d}\Omega_2\,\mathrm{d}E_1}\right|_{\downarrow}. \tag{18}$$

Here the symbols ($\uparrow$) and ($\downarrow$) denote 'up' and 'down' orientation. Obviously, the MD is proportional to the tensor $|\bar{\rho}_{10}|$ of the target and only the terms with $k_0 = 1$ in the sum (12) contribute to MD. These terms involve the dynamical coefficients $B^{k_1k_2}_{1kk_\gamma}$. MD exists both for circularly (CMD) and linearly (LMD) polarized photons.

It is important to underline that in general the measurements of CD and CMD yield different results [22]. For the CD not only the orientation of the target is important but also its alignment. In contrast, the alignment contribution does not change the sign when the target orientation direction is inverted and hence such a contribution is not present in CMD. On the other side, the CMD contains contributions from the second rank statistical tensor of the photon ($k_\gamma = 2$), whereas such terms are irrelevant for CD. Nevertheless, as shown below, for some kinematical arrangement of the PDI experiment the CD and CMD may coincide. If the main goal of the experiment is to study the chiral properties of the target, one should choose a geometry in which the kinematical dichroism vanishes i.e. non-chiral kinematics. In these

cases the final-state chirality of the emitted electron pair is zero, and therefore $k =$ even. Then in our illustrative case of $J = 1$ we conclude the following: the relevant terms for the CMD are only $B_{101}^{k_1k_2}$, $B_{121}^{k_1k_2}$ and $B_{122}^{k_1k_2}$ whereas for CD only $B_{101}^{k_1k_2}$, $B_{121}^{k_1k_2}$ and $B_{221}^{k_1k_2}$ are important. By choosing the target polarization to be along the photon beam (z-axis), the properties of the Clebsch–Gordan coefficients contained in $F_{k_0kk_\gamma}^{k_1k_2}$ dictate that $k + k_0 + k_\gamma =$ even. Since k is even, we deduce that $k_0 + k_\gamma$ should be also even. Hence, in this case both CD and CMD are determined by only two dynamical coefficients $B_{101}^{k_1k_2}$ and $B_{121}^{k_1k_2}$, and therefore they are equal, meaning that inverting the chirality of the light is equivalent to flipping the target polarization direction. This fact is comprehensible from a simple geometrical consideration (see section 5).

3.3. Linear alignment dichroism

We consider now the case where the target is aligned. The difference in the cross sections of PDI for linearly polarized light with two orthogonal axis of the target alignment constitutes the linear alignment dichroism.

$$\mathrm{LAD} = \left.\frac{\mathrm{d}^3\sigma}{\mathrm{d}\Omega_1\,\mathrm{d}\Omega_2\,\mathrm{d}E_1}\right|_{\parallel} - \left.\frac{\mathrm{d}^3\sigma}{\mathrm{d}\Omega_1\,\mathrm{d}\Omega_2\,\mathrm{d}E_1}\right|_{\perp}. \tag{19}$$

For LAD only terms with $k_0 = 2$ in the sum (12) are relevant. The dynamical coefficients contributing to LAD are $B_{2kk_\gamma}^{k_1k_2}$. The expression for the angular distribution of LAD simplifies if the alignment axis coincides with the linear polarization axis of the ionizing radiation, a case which will be discussed in section 5 using numerical illustrations. Generally, LAD persists even upon an integration over the angles of one of the electrons and even in the total cross section, in which case the quantity of interest would be the dependence of the total cross section on the angle between the photon polarization direction and the alignment axis [21, 30].

4. Physical significance of the circular dichroism in PDI

4.1. Plane wave approximation

For understanding qualitatively the general features of the PDI cross sections from polarized targets, it is instructive to consider a simple analytic approximation for the continuum two-electron final-state wavefunction such as the plane wave approximation. Generally, the PWA is not a useful method for describing quantitatively PDI from atomic targets, unless the electron energies are high as compared to the two-electron initial binding energy (strictly speaking the PWA is never exact for scattering potentials that involve an infinitely long-range tail, such as Coulomb potentials). In solids where naturally (orbitally) ordered state may occur, the direct electron–electron repulsion is screened on the scale of a few lattice constants. This feature extends the validity of the PWA beyond the range, typically assumed in atomic scattering processes.

To exploit the advantages of the PWA we consider at first the dipole amplitude $\mathbf{f}(\mathbf{p}_1, \mathbf{p}_2)$, as given by equation (3). The dipole operator does not act in spin space. In addition, we study the cases where the detectors are not sensitive to electron spins, therefore the PDI cross section is not explicitly spin dependent. Nevertheless, the initial two electron spin state of the target has a crucial influence in that it determines the symmetry of the spacial part of the electron wavefunctions. Keeping this in mind we omit the spin variables in the formulae to shorten notations.

Similarly to [1] we consider the partial two-electron Fourier amplitude $\tilde{\Psi}_{if}(\mathbf{q}_1, \mathbf{q}_2)$ of the many electron wavefunction $\Psi_{J_0M_0}(\mathbf{r}_1, \ldots, \mathbf{r}_n)$ projected on a selected state $\Psi_{J_fM_f}(\mathbf{r}_3, \ldots, \mathbf{r}_n)$ of the final doubly charged ion. These amplitudes are given by the formulae

$$\tilde{\Psi}_{\mathrm{if}}(\mathbf{q}_1, \mathbf{q}_2) = (2\pi)^{-3} \int \mathrm{d}\mathbf{r}_1\, \mathrm{d}\mathbf{r}_2 \Psi_{\mathrm{if}}(\mathbf{r}_1\mathbf{r}_2)\, \exp(-\mathrm{i}(\mathbf{q}_1 \cdot \mathbf{r}_1 + \mathbf{q}_2 \cdot \mathbf{r}_2)), \tag{20}$$

where

$$\Psi_{\mathrm{if}}(\mathbf{r}_1, \mathbf{r}_2) = \int \Psi_{J_0M_0}(\mathbf{r}_1, \ldots, \mathbf{r}_n)\Psi_{J_fM_f}(\mathbf{r}_3, \ldots, \mathbf{r}_n)^*\, \mathrm{d}\mathbf{r}_3, \ldots, \mathrm{d}\mathbf{r}_n. \tag{21}$$

Within the PWA and employing the length form for the dipole operator, the amplitude $\mathbf{f}(\mathbf{p}_1, \mathbf{p}_2)$ can be written as

$$\mathbf{f}(\mathbf{p}_1, \mathbf{p}_2) = \mathrm{i}\nabla \tilde{\Psi}_{\mathrm{if}}(\mathbf{p}_1, \mathbf{p}_2). \tag{22}$$

Here we introduced the total gradient $\nabla = \nabla_{\mathbf{p}_1} + \nabla_{\mathbf{p}_2}$. In equation (22), the momenta $\mathbf{p}_1$ and $\mathbf{p}_2$ are determined experimentally. Thus, by measuring the cross section at certain $\mathbf{p}_1$ and $\mathbf{p}_2$, the modulus square of the wavefunction gradient can be measured (or projected) at certain momentum–space subregions defined by $\mathbf{p}_1$ and $\mathbf{p}_2$. If the system under study consists of a two-electron atom or ion then $\tilde{\Psi}_{\mathrm{if}}(\mathbf{p}_1, \mathbf{p}_2) \equiv \tilde{\varphi}_{\mathrm{i}}(\mathbf{p}_1, \mathbf{p}_2)$ where $\tilde{\varphi}_{\mathrm{i}}(\mathbf{p}_1, \mathbf{p}_2)$ is the momentum–space wavefunction of the initial state of the atom.

To elucidate the properties of the circular dichroism in PDI, as calculated within the PWA, we write at first the modulus square of the transition amplitude as $|T_{\hat{\epsilon}_\pm}|^2 = (\hat{\boldsymbol{\epsilon}}_\pm \cdot \mathbf{f})(\hat{\boldsymbol{\epsilon}}_\pm^* \cdot \mathbf{f}^*)$. The terms in the double product can be rearranged and one obtains that

$$|T_{\hat{\epsilon}_\pm}|^2 = \tfrac{1}{3}|\mathbf{f}|^2 + \tfrac{1}{2}(\hat{\boldsymbol{\epsilon}}_\pm \times \hat{\boldsymbol{\epsilon}}_\pm^*) \cdot (\mathbf{f} \times \mathbf{f}^*) + \mathrm{T}_2(\hat{\boldsymbol{\epsilon}}_\pm, \hat{\boldsymbol{\epsilon}}_\pm^*)\mathrm{T}_2(\mathbf{f}, \mathbf{f}^*). \tag{23}$$

Here $\mathrm{T}_2(\mathbf{x}, \mathbf{y})$ is a spherical tensor of rank 2 constructed from the spherical components of the vectors $\mathbf{x}$ and $\mathbf{y}$ [28]. Only the second term on the rhs of equation (23) is odd with respect to exchange of $\hat{\boldsymbol{\epsilon}}_+$ and $\hat{\boldsymbol{\epsilon}}_-$ (or $\mathbf{f}$ and $\mathbf{f}^*$). Therefore, the measurable circular dichroism CD, defined in equation (17), can be rewritten as

$$\mathrm{CD} = c[|T_{\hat{\epsilon}_+}|^2 - |T_{\hat{\epsilon}_-}|^2] = -\mathrm{i}c\hat{\mathbf{n}}_\gamma \cdot (\mathbf{f} \times \mathbf{f}^*), \tag{24}$$

where $\hat{\mathbf{n}}_\gamma = \pm\mathrm{i}\hat{\boldsymbol{\epsilon}}_\pm \times \hat{\boldsymbol{\epsilon}}_\pm^*$ is a real unit vector along the light propagation direction. The vector product $\mathbf{f} \times \mathbf{f}^*$ is pure imaginary, because $\mathbf{f} \times \mathbf{f}^* = -(\mathbf{f} \times \mathbf{f}^*)^*$. Therefore, no circular dichroism exists if $\mathbf{f}$ is pure real or pure imaginary. It should be stressed that equation (24) and the related conclusions are generally valid, i.e. they are not restricted to the PWA and apply without special symmetry requirements on the system under investigation. Introducing the PWA amplitude (22) and using equations (20) and (24) we get

$$\mathrm{CD} = -\mathrm{i}c\hat{\mathbf{n}}_\gamma \cdot [\nabla \tilde{\Psi}_{\mathrm{if}}(\mathbf{p}_1, \mathbf{p}_2) \times \nabla \tilde{\Psi}^*_{\mathrm{if}}(-\mathbf{p}_1, -\mathbf{p}_2)]. \tag{25}$$

We recall that the spin degrees of freedom are assumed to be decoupled from the spacial ones. In this case a time-reversal operation Θ acting on the two-electron wavefunction leads to the result $\Theta\tilde{\Psi}_{\mathrm{if}}(\mathbf{p}_1, \mathbf{p}_2) = \tilde{\Psi}^*_{\mathrm{if}}(-\mathbf{p}_1, -\mathbf{p}_2)$. Therefore, relation (25) evidences that CD changes its sign upon time reversing the two-electron bound states and hence CD vanishes when the initial state is a time-reversal invariant. In this sense a finite CD can be regarded as an indicator for a broken time-reversal symmetry [43]. This break of symmetry can be brought about experimentally, e.g. by orbitally polarizing the initial state via laser pumping. On the other hand there are a variety of examples of naturally occurring (spontaneous) time-reversal symmetry breaking (see section 6). We note by passing that a sign reversal of the phase of the position space wavefunction of the bound state $\Psi_{\mathrm{if}}(\mathbf{r}_1, \mathbf{r}_2)$ corresponds to reversing sign of the phase of the momentum–space wavefunction and reversing the direction of the momenta, i.e. $\Psi_{\mathrm{if}}(\mathbf{r}_1, \mathbf{r}_2) \mapsto \Psi^*_{\mathrm{if}}(\mathbf{r}_1, \mathbf{r}_2)$ corresponds to $\tilde{\Psi}_{\mathrm{if}}(\mathbf{p}_1, \mathbf{p}_2) \mapsto \tilde{\Psi}^*_{\mathrm{if}}(-\mathbf{p}_1, -\mathbf{p}_2)$.

This is readily concluded from equation (20). Thus, CD changes sign upon the operation $\Psi_{\mathrm{if}}(\mathbf{r}_1, \mathbf{r}_2) \mapsto \Psi^*_{\mathrm{if}}(\mathbf{r}_1, \mathbf{r}_2)$. A classical analogue of the phase of the wavefunction is the circulation direction of the charge carriers with respect to a given axis (direction of orientation). Changing sign of the phase amounts to reversing the direction of circulation. This is shown explicitly below (cf equation (32)).

To proceed further we express the momentum–space wavefunction of the electron pair as

$$\tilde{\Psi}_{\mathrm{if}}(\mathbf{p}_1, \mathbf{p}_2) = |\tilde{\Psi}_{\mathrm{if}}(\mathbf{p}_1, \mathbf{p}_2)|\, \mathrm{e}^{\mathrm{i}\phi(\mathbf{p}_1, \mathbf{p}_2)}, \tag{26}$$

where $\phi(\mathbf{p}_1, \mathbf{p}_2)$ is the phase of the wavefunction. Comparing equations (22), (24) and (26) we conclude that within the PWA

$$\begin{aligned} \mathrm{CD} &\equiv \sigma(\hat{\boldsymbol{\epsilon}}_+, \phi) - \sigma(\hat{\boldsymbol{\epsilon}}_-, \phi) = \sigma(\hat{\boldsymbol{\epsilon}}_+, \phi) - \sigma(\hat{\boldsymbol{\epsilon}}_+, -\phi) \\ &= \sigma(\hat{\boldsymbol{\epsilon}}_-, -\phi) - \sigma(\hat{\boldsymbol{\epsilon}}_-, \phi). \end{aligned} \tag{27}$$

The following key conclusions are based on the relations (27). The circular dichroism can be regarded as a measurable change in the PDI cross section (for circularly polarized light of a fixed helicity) upon a sign reversal of the phase of the initial-state two-electron momentum–space wavefunction. For non-oriented two-electron atom the initial-state wavefunction may be chosen to be real $\phi \equiv 0$ and hence $\mathrm{CD} = 0$. This is consistent with the statement that for isotropic initial state CD vanishes identically within the PWA proved in [9]. In general, however, CD is nonzero for PDI from unpolarized targets [9] apart from the conditions of non-chiral kinematics as discussed in section 2.

Within the PWA it is also possible to derive a direct link between the circular dichroism and the phase difference (gradient) of the electron pair wavefunction: Inserting equation (26) into equations (22) and (24) yields

$$\mathrm{CD} = c\{(\boldsymbol{\nabla}|\tilde{\Psi}_{\mathrm{if}}(\mathbf{p}_1, \mathbf{p}_2)|^2) \times \hat{\mathbf{n}}_\gamma\} \cdot \boldsymbol{\nabla}\phi(\mathbf{p}_1, \mathbf{p}_2). \tag{28}$$

In this context we recall that a way to obtain information related to the two-particle probability density $|\tilde{\Psi}_{\mathrm{if}}(\mathbf{p}_1, \mathbf{p}_2)|^2$ by means of PDI was, to our knowledge, first discussed in [1] (in the context of atomic physics). The measurements of CD give access to phase differences (gradient) of the bound two-particle state [43].

4.2. Beyond PWA

The discussion following equation (25) highlighted the fact that CD changes sign upon a time reversal of the electron-pair state. Time reversal corresponds to a change of the phase sign of the position-space bound-state wavefunction of electron pair. Therefore, CD changes the sign upon the operation $\Psi_{\mathrm{if}}(\mathbf{r}_1, \mathbf{r}_2) \mapsto \Psi^*_{\mathrm{if}}(\mathbf{r}_1, \mathbf{r}_2)$. This result we have obtained within the PWA. Now we demonstrate its validity for the general case, provided a particular kinematical condition of the experiment is chosen. The transformation $\Psi_{\mathrm{if}}(\mathbf{r}_1, \mathbf{r}_2) \mapsto \Psi^*_{\mathrm{if}}(\mathbf{r}_1, \mathbf{r}_2)$ implies a complex conjugation of the density operator of the initial state, i.e. $\rho^i(J_0) \mapsto \rho^{i*}(J_0)$. The substitution into equation (6) shows that the statistical tensors transform as $\rho_{k_0 q_0}(\alpha_0 J_0) \mapsto (-1)^{k_0} \rho_{k_0 q_0}(\alpha_0 J_0)$. Thus, upon a phase sign change of the initial state wavefunction (i.e. upon time reversal in the initial state) the orientation ($k_0 = 1$) changes the sign while the alignment ($k_0 = 2$) does not change. In section 3.1 we have shown that in an experiment with a non-chiral kinematics when the direction of the photon beam coincides with the target polarization direction, the alignment does not contribute to the CD. In this kinematical conditions the CD is proportional to the target orientation $\bar{\rho}_{10}$ and thus it changes the sign when the phase of the bound-state function changes its sign.

5. Example: photo-double ionization of polarized 2P state of He

To illustrate the above findings we consider a simple example, namely PDI from a polarized He atom. The ground state of He has $J_0 = 0$ and cannot be polarized. However, the excited states $2\,^{1,3}$P can be polarized, e.g. by pumping with circularly or linearly polarized laser one achieves respectively an oriented or an aligned two-electron states. Experimentally, the use of the excited He as a target is not a major obstacle at least for the comparatively long-living 2^3P state. The feasibility of excited He target for scattering experiments was demonstrated, for example, in [44], where superelastic electron scattering was studied from laser excited 2^3P He state. PDI from excited (but not polarized) He atoms has been recently considered theoretically in [45, 46]. Below we present the results of calculations for PDI of excited and polarized He 2P states. To make the presentation and the interpretation of the results more transparent we choose the laboratory coordinate system such that the z-axis coincides with the photon beam propagation direction for circularly polarized light or with the photon polarization for linearly polarized light. The properties of the kinematical dichroism have been well established previously [37]. Therefore, to focus on the new target-polarization effects we eliminate the kinematical dichroism by choosing a coplanar geometry: the plane spanned by the momenta $\mathbf{p}_1$ and $\mathbf{p}_2$ of the emitted electrons contains the z-axis. Furthermore, we consider the case in which the He atom is polarized along the z-axis.

We describe the spacial part $\varphi_m(\mathbf{r}_1, \mathbf{r}_2)$ of the He 2P states with the orbital angular momentum projection m as (anti)symmetrized product of two hydrogen-like single-electron wavefunctions u_{nl} with effective charges considered as variational parameters, i.e.

$$\varphi_m(\mathbf{r}_1, \mathbf{r}_2) = N_\pm[u_{1s}(r_1)u_{2p}(r_2)Y_{1m}(\hat{\mathbf{r}}_2) \pm u_{1s}(r_2)u_{2p}(r_1)Y_{1m}(\hat{\mathbf{r}}_1)], \tag{29}$$

where $N_\pm$ is a normalization factor. The + (−) sign refers to the singlet 2^1P (triplet 2^3P) state. For the 2^1P state the values of the variational parameters are $Z_{1s} = 2$ and $Z_{2p} = 0.97$ [47] which gives a binding energy of $E(2^1\mathrm{P}) = -2.123$ (experimental value is -2.124). For the 2^3P state one finds $Z_{1s} = 1.99$ and $Z_{2p} = 1.09$ [47] leading to the binding energy of $E(2^3\mathrm{P}) = -2.131$ (experimental value is -2.133). Thus, the wavefunctions (29) are simple, but reasonable starting point for pilot calculations of PDI cross sections and dichroism.

The final state of the two electrons in the continuum is approximated by a product of two plane waves multiplied by three two-body Coulomb distortion factors describing the separate interaction of each electron with the residual ion and electron–electron interaction, the so-called 3C-approximation [9, 48, 49]. The advantages and disadvantages of the 3C approximation as applied to PDI have been discussed in the review [2] together with other analytical and numerical approaches. The 3C wavefunction has a number of weak points (a detailed mathematical analysis of the shortcomings of the 3C model can be found in [50]), but it is probably fair to say that the 3C approximation captures the main features of the two-particle continuum and hence is well suited for our purposes here. With these final-state wavefunctions, calculations of the amplitudes $\mathbf{f}(\mathbf{p}_1, \mathbf{p}_2)$ and of the cross sections have been done full-numerically on a six-dimensional grid (for the results shown here, the cut-off for the radial integration was at about 50 au, where convergence was achieved). For comparison and for testing the numerics we made also calculations within the PWA.

At first we consider the results of the calculations for circularly polarized light. Figure 1 presents the calculated cross sections for He 2^1P state for different projections of the angular momentum m and different photon helicities $\epsilon_\pm$. The cross sections are shown as a function of the emission angle of the second electron while the emission direction of the first electron is fixed along the z-axis (see insets in figure 1). In this case three of four vectors, characterizing the process $\hat{\mathbf{a}}$, $\hat{\mathbf{n}}_\gamma$ and $\hat{\mathbf{n}}_\mathbf{1}$ are collinear, and as it was proved in section 3 the CD and CMD should

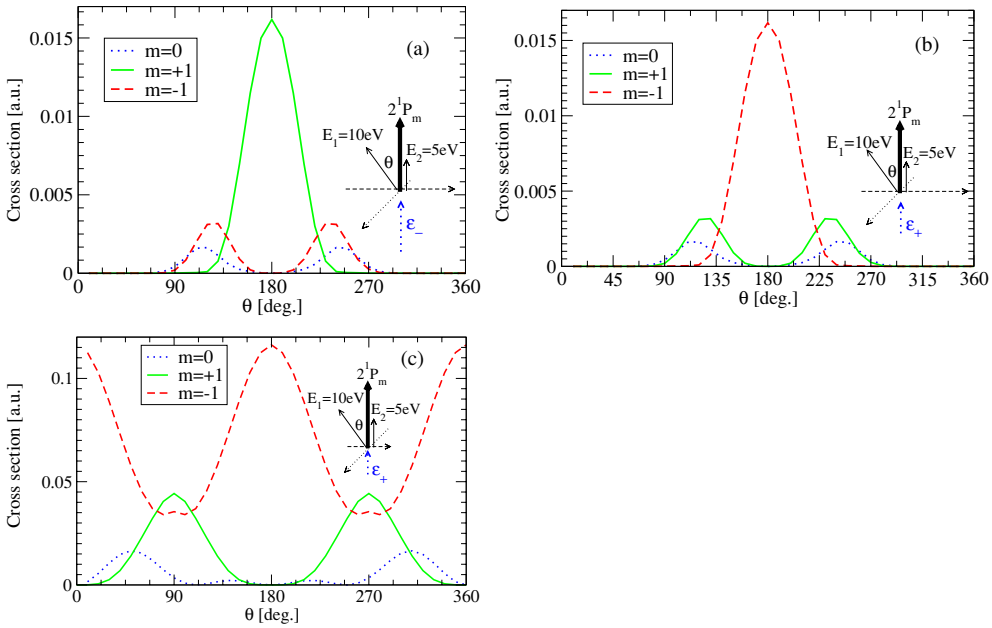

Figure 1. m-resolved double ionization cross section of the 2^1P_m state of atomic helium following the absorption of a right (left) circularly polarized photon, labelled respectively by ϵ_+ (ϵ_-). The polar angle θ of the first 10 eV electron is varied. The emission angle of the second, slow electron with 5 eV energy is fixed along the light propagation direction (which is also the quantization axis of the atom (thick arrow)). The calculations were done using the 3C model for left (a) and right (b) circularly polarized light and within PWA for right circularly polarized light (c).

coincide, which means that the inversion of the photon helicity is equivalent to the inversion of orientation (sign of the projection m). This can easily be proved also from symmetry point of view. Indeed, in the chosen geometry the angular distribution of the second electron ($\hat{\mathbf{n}}_2$) should be axially symmetrical about the z-axis. A reflection of the system through a plane containing the z-axis results in the change of the photon helicity $\boldsymbol{\epsilon}_+ \to \boldsymbol{\epsilon}_-$ and of the angular momentum projection $m \to -m$. On the other hand, due to axial symmetry the cross section should be invariant under the rotation about the z-axis at 180°, therefore

$$\sigma(\boldsymbol{\epsilon}_+, m) = \sigma(\boldsymbol{\epsilon}_-, -m) \tag{30}$$

Naturally, numerical calculations confirm this relation (cf figures 1(a) and (b)). As seen from the figure the circular dichroism is very strong for $m = \pm 1$ states, the non-chiral $m = 0$ state shows no dichroism. The angular distributions differ drastically for different m. It is interesting to compare the results of the 3C calculations with those made within PWA (cf figures 1(b) and (c)). One can see that apart from the values of the cross sections, the characters of the curves are similar in the backward hemisphere. However in the forward hemisphere Coulomb repulsion of electrons moving in close directions strongly suppresses the cross sections.

The striking difference in the angular distributions for the different projections m can be qualitatively understood within the single configuration approximation which we use for the description of He. Consider, for example, PDI of He 2P by right-circularly polarized light $\boldsymbol{\epsilon}_+$. One of the electrons absorbs the photon and the dipole transitions $1s \to Ep$ or $2p \to Es, Ed$ can occur. The second electron is 'shaken' to the continuum with the same angular momentum: $2p \to Ep$ in the former case and $1s \to Es$ in the latter case. Therefore, in the continuum

we may have the following electron pairs (channels) (p,p), (s,s) and (s,d). Photoabsorption of the right-circularly polarized light involves a change of the angular momentum projection $\Delta m = +1$. If we consider the ionization of the state $m = +1$, the final-state projection should be $m_f = +2$. Since one of the electrons emitted along the z-axis has zero projection, the second one should have projection +2. The only contributing channel (s,d) gives angular distribution of the type $\sin^4\theta$ strongly peaked at 90° and 270°. This is valid for PWA (non-interacting electrons), see figure 1(c). Final-state interaction shifts the maxima, but the character of the distribution remains the same (figure 1(b)). If the initial state has $m = 0$ the final state should have projection $m_\mathrm{f} = +1$. In both possible channels (p,p) and (s,d) the angular wavefunctions have zeros at 0° and 180°. Since the dominant dipole transition is 2p $\rightarrow$ Ed, the main contribution to the angular distribution comes from $|Y_{2\pm1}|^2$ function that has additionally zeros at 90° and 270° which explains the observed angular distribution. Finally, for the ionization of the $m = -1$ state, the final state has $m_\mathrm{f} = 0$. In all three channels it gives maxima at 0° and 180° (see figure 1(c)). Final-state interaction eliminates the 0° peak, but the peak at 180° persists (see figure 1(b)).

Using the results of figure 1 we can predict the results of CD and CMD measurements. First we note that in equation (29) m is the projection of the angular momentum of the two-electron wavefunction onto the axis of quantization (z-axis). According to the definition (6) for $J_0 = 1$ the orientation tensor $\rho_{10}(1)$ is expressed as

$$\rho_{10}(1) = \tfrac{1}{\sqrt{2}}(w_{+1} - w_{-1}) \tag{31}$$

where w_m is a population of the magnetic substate with projection m. Thus if only one of the projections $m = \pm1$ is populated, the *electron-pair* state is maximally oriented along the $\pm z$ direction, $\rho_{10}(1) = \pm\sqrt{1/2}$. If only $m = 0$ is populated, the state is non-oriented. With the account of equation (30) the circular dichroism for the maximally oriented target can be expressed as

$$\begin{aligned}\mathrm{CD} = \mathrm{CMD} &= \sigma(\boldsymbol{\epsilon}_+, m) - \sigma(\boldsymbol{\epsilon}_-, m) = \sigma(\boldsymbol{\epsilon}_+, m) - \sigma(\boldsymbol{\epsilon}_+, -m) \\ &= \sigma(\boldsymbol{\epsilon}_-, -m) - \sigma(\boldsymbol{\epsilon}_+, m) = \sigma(\boldsymbol{\epsilon}_-, -m) - \sigma(\boldsymbol{\epsilon}_-, m).\end{aligned} \tag{32}$$

These relations are the counterparts to equations (27) obtained above within PWA; here they are valid for any correlated final continuum state but only in a special case of non-chiral kinematics. Figure 2 shows the CD calculated according to (32). The lobe structure of the CD is explained by the extremal values of the corresponding cross sections.

In figure 3 we show the results similar to those in figure 1(a) but for the triplet initial state ^{3}P. The large difference between PDI cross sections from triplet and singlet states demonstrates the high sensitivity of the dichroism in PDI to the electron–electron correlations (in this case, correlations due to the exchange interaction).

Now let us consider PDI by linearly polarized light. In this case we chose the z-axis along the light polarization. The geometry of the experiment is shown in the inset in figure 4 where the results of the calculations are shown for He 2P initial state. In the chosen geometry and for linearly polarized light $\Delta m = 0$ applies. Therefore, in $\sigma(\epsilon_0, m = 0)$ only substates of the electron pair with $m_\mathrm{f} = 0$ can contribute. Thus according to the above consideration, if the electron interaction is ignored one can expect maxima of the cross section at 0° and 180°. The maximum in forward direction is completely suppressed by the Coulomb repulsion of electrons, but the maximum at the 'back-to-back' emission persists (see figure 4(a)). In contrast, for $\sigma(\epsilon_0, m = \pm1)$ only the states with $m_\mathrm{f} = \pm1$ contribute. In this case we can expect zero at 180° as it is obtained by the calculations. In figure 4(b) analogous results but calculated within the PWA are presented. As in the previous case of circularly polarized light, the cross-section behaviour in the backward hemisphere is similar for both calculations, while

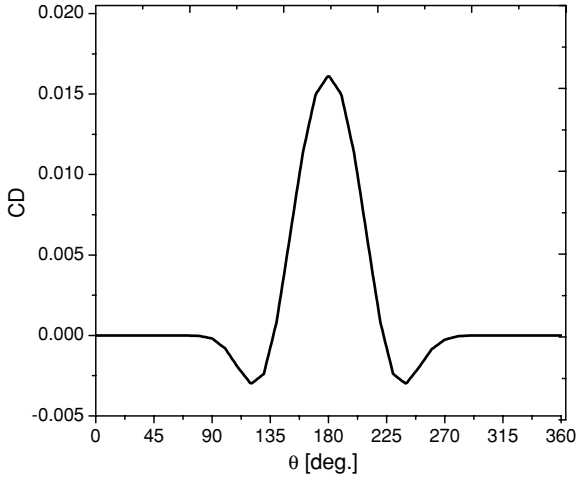

Figure 2. The circular dichroism (CD) for the scattering geometry, as depicted in the inset of figure 1(a). In this case, CD is also equivalent to the CMD as explained in the text.

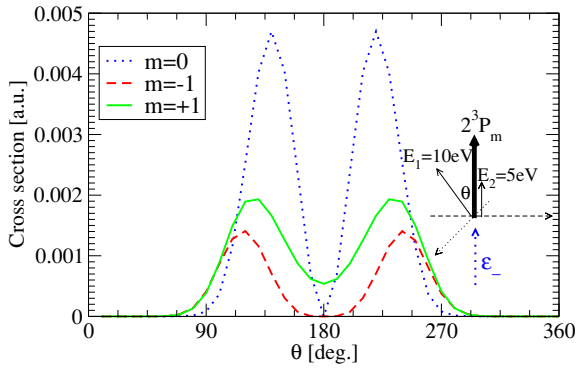

Figure 3. The same as in figure 1(a), but for the triplet state 2^3P_m of He. The results for $\hat{\epsilon}_+$ can be obtained from those shown in the figure applying equation (32).

in the forward hemisphere the Coulomb repulsion of the emitted electrons suppresses strongly the cross section in the 3C calculation (as compared to the PWA ones). Figure 4(c) presents the results of the 3C calculation for the He 2^3P initial state. Again comparing figures 4(a) and (c) we see a strong difference between the cross sections of PDI from singlet and triplet initial states that implies a strong sensitivity of the dichroism to electron correlations in the initial state.

With linearly polarized light, one can probe the alignment of the electron pair in the target. The alignment tensor of the He 2P state is defined as (cf equation (6))

$$\rho_{20}(1) = \tfrac{1}{\sqrt{6}}(w_{+1} + w_{-1} - 2w_0). \tag{33}$$

Thus if $m = \pm 1$ substates are equally populated and $w_0 = 0$ the alignment is $\rho_{20}(1) = +\sqrt{2/3}$, while if only $m = 0$ is populated the alignment is $\rho_{20}(1) = -\sqrt{2/3}$. Note that the rotation of the quantization axis by 90° around the y-axis exchanges the alignment of the above two states. In section 3.3 we have defined linear alignment dichroism as the difference of the cross

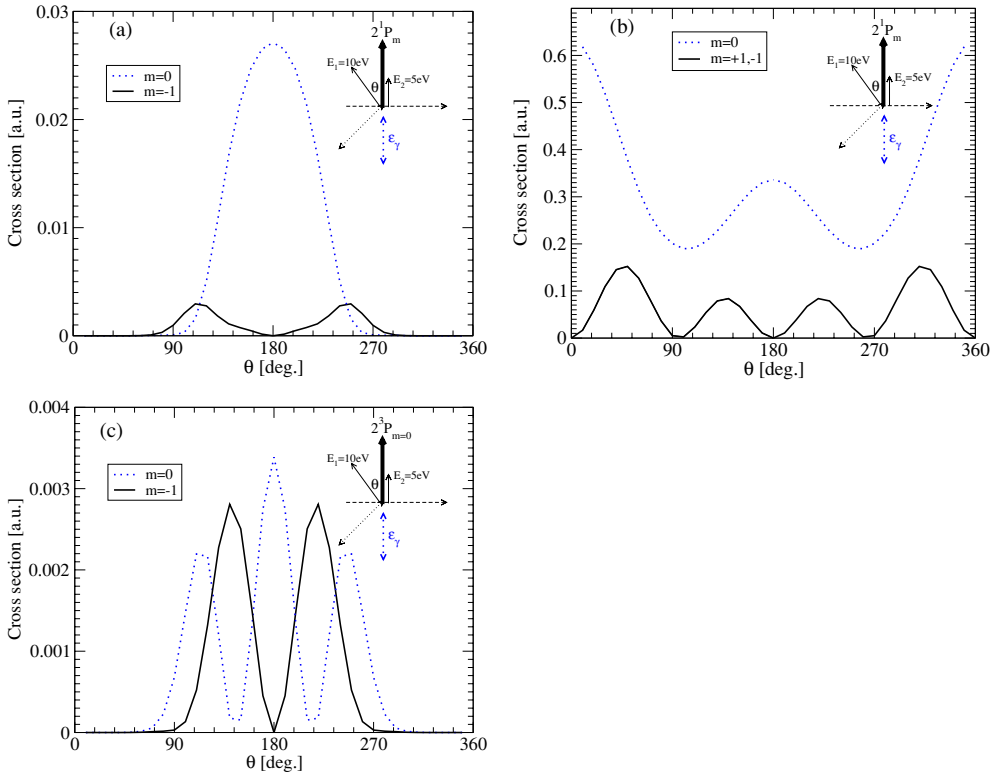

Figure 4. The fully differential cross section for the double ionization of He with linearly polarized light. The photon polarization axis is chosen to be along the atom quantization axis. Energies and scattering angles depicted in the insets are the same as in figure 1. The calculations were done for the singlet 2^1P_m initial states using 3C model (a) and PWA (b) and for the triplet 2^3P_m initial states using 3C model (c). In (b) the results for the states $2^1P_{m=\pm1}$ are multiplied by a factor 8.

sections for two perpendicular axis of alignment. One can show that LAD for $L = 1$ state may be expressed in terms of the cross sections $\sigma(\epsilon_0, m)$ as

$$\text{LAD} = \sigma(\epsilon_0, m = \pm 1) - \sigma(\epsilon_0, m = 0). \tag{34}$$

Figure 5 presents the calculated LAD for the ionization of the $2^{1,3}$P states of He in the geometry shown in the inset. As for the CD, the LAD angular dependence shows lobes which are determined by the extrema of the cross sections.

6. Possible applications to superconductors and other materials

The above discussion of the PDI and the circular dichroism was mainly concentrated on atomic targets. However, the main ideas and results outlined here can as well be applied to other systems. In this section we outline briefly some applications of the theory of circular dichroism in PDI or better to say in double-photo emission to the study of unconventional superconductors.

It is established knowledge that the inter-quasiparticle interactions are the driving force behind spontaneous symmetry breaking and the formation of new states of matter, such as ferromagnetism and superconductivity (SC) [51–53]. In conventional SC the gauge symmetry

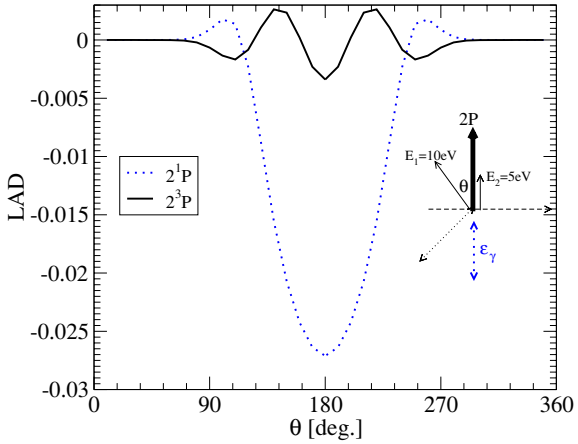

Figure 5. Linear alignment dichroism (LAD) evaluating according to equation (34). The scattering geometry and the energies of the two escaping electrons are shown in the inset (same as in figure 4).

is broken at the critical temperature T_c [51] due to the formation of (s-wave) Cooper pairs with a vanishing total spin. The order parameter Δ, i.e. the pair wavefunction in momentum–space is then isotropic $\Delta = \Delta_0$. A recent work [16] demonstrated that PDI is capable of mapping out some details of the correlation within a Cooper pair in a conventional s-wave SC. With the findings of the present work we show now that PDI is as well instrumental in unravelling the interplay between correlation and other type of spontaneous symmetry breaking, in particular the break of the time-reversal symmetry.

The gauge symmetry is broken for all kind of SCs underpinned by a pairing mechanism. On the other hand, new states of unconventional SC associated with other kind of spontaneous symmetry breaking have recently been identified [51]. For instance, in the case of triplet p-wave SC, which is believed to occur in the layered $Sr_2\,RuO_4$ compound [51] (the layers are built out of Ru and O_4, similar to the Cu–O_2 layers in cuprates), the time-reversal symmetry is broken. For $T \leqslant T_c$ the superconducting ground state is called the *chiral* or the Anderson–Brinkmann–Morel (ABM) phase [51, 53]. The pairing state is specified by the so-called **d** vector order parameter: $\mathbf{d} = \Delta_0\hat{\mathbf{z}}(k_x \pm \mathrm{i}k_y) = \Delta_0(0, 0, k_x \pm \mathrm{i}k_y)$. k_x and k_y are wave vectors in the planes. The z direction is pinned along the crystalline c axis, i.e. perpendicular to the (Ru, O_4) plane[4]. The triplet paired spins are within the two-dimensional (Ru,O_4) plane, while all orbital angular momentum vectors are perpendicular to this plane and parallel to one another in any domain. The orbital wavefunction is expressible in terms of the spherical harmonics $Y_{1,\pm1} = \left(\frac{3}{8}\pi\right)^{1/2} \sin\theta\, \mathrm{e}^{\pm\mathrm{i}\phi} = \left(\frac{3}{8}\pi\right)^{1/2}(k_x \pm \mathrm{i}k_y)$. Thus, the relative orbital motion of the electrons of a Cooper pair is either clockwise or counterclockwise. The fact that all the Cooper pairs within a given superconducting domain follow the same sense of the (orbital) rotation underpins the broken time-reversal symmetry. As proved above, generally measuring CD in PDI in the non-chiral kinematics can be utilized as an indicator of the time-reversal symmetry breaking. More detailed information can be gained if we assume that the final state is well approximated by plane waves. As showed in section 4, we can utilize the angular dependence of the CD to infer information on the angular behaviour of the pair phase gradient.

[4] The pinning of the z-direction along the crystalline c-axis of the highly anisotropic Sr_2RuO_4 crystal is brought about by a weak spin–orbit coupling (SOC). It should be noted however that SOC in these materials is nevertheless not as large as to invalidate a decoupling of the spin from the orbital degrees of freedom.

As for the validity of the PWA in this case we note that the coherence length, i.e. the extent of the pair state, is estimated to be ~ 1000 Å. Thus we can argue that due to screening a PWA for the excited (broken) pairs is well justifiable.

In this context we recall that the signature of a broken time-reversal symmetry is as well present in a single photoemission measurement (as demonstrated experimentally for the pseudogap state of high T_c SCs [54]). It should be remarked however that single photoemission tests for the symmetry of single particle orbitals (integrated over all other degrees of freedom of the surrounding medium). PDI is related to the properties of electron *pairs*. This is explicitly demonstrated in the numerical examples, where a triplet-oriented pair leads to a markedly different CD than a singlet-paired state. Hence, CD and PDI measurements supersede single photoemission in that they allow an insight into the interplay between symmetry reduction and inter-particle correlation. A concrete numerical demonstration of these statements for high T_c SCs will be presented elsewhere [55].

Another important class of materials that can be potentially investigated by PDI are systems with a natural orbital ordering [56]. As for unconventional superconductors these materials are of great practical importance, but the underlying physics is still to be established. As demonstrated in this paper a measurement of the CD (in the non-chiral kinematics) may serve as an indicator for the presence of a preferential orientation axis of the orbital motion. In addition, PDI provides direct information on the short-range correlations (note the electron–electron interaction which triggers PDI is usually screened on the scale of few tens of angstroms).

7. Conclusions

We have presented and analysed a general expression for the triple differential cross section of the photo-double ionization of polarized atoms. The cross section reveals different kinds of dichroism including magnetic and circular dichroism. It is shown that circular dichroism is a combination of a polarization dichroism connected with the polarization of the target and a kinematical dichroism caused by the choice of experimental geometry. For studying the dichroism caused by the intrinsic chirality of the target, it is necessary to make experiments in conditions where kinematical dichroism vanishes, for example in coplanar kinematics. Further analysis of the circular dichroism in PDI has revealed that a finite CD carries information on the properties of the phase of the bound two-particle wavefunction. The calculations of the PDI cross sections from polarized helium have demonstrated that PDI in combination with the dichroism measurements give access to the internal (phase) properties of bound two-electron states. The realization of the suggested experiments might be an experimental challenge, however the information attainable is unique in that it reveals the interrelation between electronic correlation and two-particle phase differences. This has been shown explicitly in this present work by revealing (theoretically) the marked difference in CD for a singlet and a triplet two-particle state, demonstrating thus the influence of the exchange interaction.

A further key conclusion of this study is that a finite CD is an indicator for a broken time-reversal symmetry. This we have shown without resorting to any special approximate expressions of the wavefunction and without assuming any particular type of symmetry for the target. This finding is of special importance for the investigation of systems with spontaneous time-reversal symmetry breaking, such as p- and d-wave superconductors. In this case the PDI is particulary suited since the symmetry break is brought about by a quasi-particle interaction that, at the critical temperature, makes the Fermi seem unstable (Cooper instability) against pairing and a reduction of symmetry occurs. PDI has then the potential to explore the interplay

between time-reversal symmetry break and the correlation within an electron pair. Thus, the PDI capability supersedes that of conventional single photoemission.

Acknowledgments

One of the authors (NMK) acknowledges the hospitality and the financial support of the Max-Planck-Institut für Mikrostrukturphysik (Halle) and of the Bielefeld University.

References

[1] Smirnov Yu F, Pavlichenkov A V, Levin V G and Neudachin V G 1978 *J. Phys. B: At. Mol. Phys.* **11** 3587
[2] Briggs J S and Schmidt V 2000 *J. Phys. B: At. Mol. Opt. Phys.* **33** R1
[3] Mazeau J, Selles P, Waymel D and Huetz A 1991 *Phys. Rev. Lett.* **67** 820
[4] Krässig B, Schaphorst S J, Schwarzkopf O, Scherer N and Schmidt V 1996 *J. Phys. B: At. Mol. Opt. Phys.* **29** 4255
[5] Beyer H-J, West J B, Ross R J and de Fanis A 2000 *J. Phys. B: At. Mol. Opt. Phys.* **33** L767
[6] Wehlitz R and Whitfield S 2001 *J. Phys. B: At. Mol. Opt. Phys.* **34** L719
[7] Maulbetsch F and Briggs J S 1993 *J. Phys. B: At. Mol. Opt. Phys.* **26** 1679
[8] Maulbetsch F and Briggs J S 1996 *J. Phys. B: At. Mol. Opt. Phys.* **29** 4127
[9] Berakdar J and Klar H 1992 *Phys. Rev. Lett.* **69** 1175
[10] Kheifets A S and Bray I 2002 *Phys. Rev.* A **65** 022708
[11] Kazansky A K, Selles P and Malegat L 2003 *Phys. Rev.* A **68** 052701
[12] Citrini F, Malegat L, Selles P and Kazansky A K 2003 *Phys. Rev.* A **67** 042709
[13] Berakdar J 1998 *Phys. Rev.* B **58** 9808
[14] Fominykh N, Berakdar J, Henk J and Bruno P 2002 *Phys. Rev. Lett.* **89** 086402
[15] Herrmann R, Samarin S, Schwabe H and Kirschner J 1998 *Phys. Rev. Lett.* **81** 2148
[16] Kouzakov K A and Berakdar J 2003 *Phys. Rev. Lett.* **91** 257007
[17] Hasegawa S J, Miyamae T, Yakushi K, Inokuchi K, Seki K and Ueno N 1998 *Phys. Rev.* B **58** 4927
[18] Reinköster A, Korica S, Prümper G, Viefhaus J, Godenhusen K, Schwarzkopf O, Mast M and Becker U 2004 *J. Phys. B: At. Mol. Opt. Phys.* **37** 2135
[19] Kidun O, Fominykh N and Berakdar J 2004 *J. Phys. B: At. Mol. Opt. Phys.* **37** L321
[20] Jacobs V L 1972 *J. Phys. B: At. Mol. Phys.* **5** 2257
[21] Klar H and Kleinpoppen H 1982 *J. Phys. B: At. Mol. Phys.* **15** 933
[22] Cherepkov N A, Kuznetsov V V and Verbitskii V A 1995 *J. Phys. B: At. Mol. Opt. Phys.* **28** 1221
[23] Kabachnik N M 1996 *J. Electron Spectrosc. Relat. Phenom.* **79** 269
[24] Thole B T and van der Laan G 1991 *Phys. Rev.* B **44** 12
Thole B T and van der Laan G 1994 *Phys. Rev.* **49** 9613
van der Laan G and Thole B T 1993 *Phys. Rev.* **48** 210
van der Laan G and Thole B T 1995 *Phys. Rev.* **52** 15355
[25] Devons S and Goldfarb L J 1957 *Handbuch der Physik* vol 42 ed S Flügge (Berlin: Springer)
[26] Blum K 1996 *Density Matrix Theory and Applications* 2nd edn (New York: Plenum)
[27] Balashov V V, Grum-Grzhimailo A N and Kabachnik N M 2000 *Polarization and Correlation Phenomena in Atomic Collisions: A Practical Theory Course* (New York: Kluwer/Plenum)
[28] Varshalovich D A, Moskalev A N and Hersonskii V K 1998 *Quantum Theory of Angular Momentum* (Singapore: World Scientific)
[29] Schmidt V 1997 *Electron Spectrometry of Atoms Using Synchrotron Radiation* (New York: Cambridge University Press)
[30] Baier S, Grum-Grzhimailo A N and Kabachnik N M 1994 *J. Phys. B: At. Mol. Opt. Phys.* **27** 3363
[31] Kabachnik N M and Schmidt V 1995 *J. Phys. B: At. Mol. Opt. Phys.* **28** 233
[32] Chandra N 1995 *Chem. Phys. Lett.* **237** 545
[33] Sen S and Chandra N 2000 *Phys. Rev.* A **62** 052702
[34] Baumgarten L, Schneider C M, Petersen H, Schäfers F and Kirschner J 1990 *Phys. Rev. Lett.* **65** 492
[35] Verweyen A, Grum-Grzhimailo A N and Kabachnik N M 1999 *Phys. Rev.* A **60** 2076
[36] Berakdar J 2002 *Czech. J. Phys.* **52** C479
[37] Berakdar J and Klar H 2001 *Phys. Rep.* **340** 473
[38] Viefhaus J *et al* 1996 *Phys. Rev. Lett.* **77** 3975

[39] Mergel V *et al* 1998 *Phys. Rev. Lett.* **80** 5301
[40] Soejima K, Danjo A, Okuno K and Yagishita A 1999 *Phys. Rev. Lett.* **83** 1546
[41] Soejima K, Shimbo M, Danjo A, Okuno K, Shigemasa E and Yagishita A 1996 *J. Phys. B: At. Mol. Opt. Phys.* **29** L367
[42] Manakov N L, Marmo S I and Meremianin A V 1996 *J. Phys. B: At. Mol. Opt. Phys.* **29** 2711
[43] Berakdar J and Kabachnik N M 2004 *Europhys. Lett.* submitted
[44] Jacka M, Hoogerland M D, Lu W, Milic D, Baldwin K G H, Bartschat K and Buckman S J 1996 *J. Phys. B: At. Mol. Opt. Phys.* **29** L825
[45] Liang F and van der Hart H W 2002 *Phys. Rev.* A **66** 031402(R)
[46] Colgan J and Pindzola M S 2003 *Phys. Rev.* A **67** 012711
[47] Eckart C 1930 *Phys. Rev.* **36** 878
[48] Maulbetsch F and Briggs J S 1995 *J. Phys. B: At. Mol. Opt. Phys.* **28** 551
[49] Brauner M, Briggs J S and Klar H 1989 *J. Phys. B: At. Mol. Opt. Phys.* **22** 2265
[50] Berakdar J 1996 *Phys. Rev.* A **53** 2314
[51] Sigrist M and Ueda K 1991 *Rev. Mod. Phys.* **63** 239
Mackenzie A P and Maeno Y 2003 *Rev. Mod. Phys.* **75** 657
Mineev V P and Samokhin K V 1999 *Introduction to Unconventional Superconductivity* (Amsterdam: Gordon and Breach)
Luke G M *et al* 1998 *Nature* **394** 558
[52] Landau L D 1956 *Zh. Eksp. Teor. Fiz.* **30** 1058
Landau L D 1957 *Sov. Phys.—JETP* **3** 920 (Engl. Transl.)
Mahan G D 1990 *Many Particle Physics* 2nd edn (New York: Plenum)
[53] Tinkham M 1996 *Introduction to Superconductivity* 2nd edn (Singapore: McGraw-Hill)
[54] Kaminski A *et al* 2002 *Nature* **416** 610
Varma C M 2000 *Phys. Rev.* B **61** R3804
[55] Kouzakov K A and Berakdar J 2004 unpublished
[56] Rao C N R, Arulraj A, Cheetham A K and Raveau B 2000 *J. Phys.: Condens. Matter* **12** R83
Ishihara S and Maekawa S 2002 *Rep. Prog. Phys.* **65** 561